AGU PUBLICATIONS

JGR

Journal of Geophysical Research: Atmospheres

RESEARCH ARTICLE
10.1002/2017JD027248

Key Points:
- New mask method isolates the cloud response to Arctic sea ice cover by restricting analysis to where sea ice cover varies
- During fall lidar observations show larger low-level liquid cloud fractions and more opaque clouds over open water than over sea ice
- During summer lidar observations show that liquid cloud fraction profiles and opaque clouds are unaffected by sea ice cover variability

Supporting Information:
- Supporting Information S1

Correspondence to:
A. L. Morrison,
ariel.morrison@colorado.edu

Citation:
Morrison, A. L., Kay, J. E., Chepfer, H., Guzman, R. & Yettella, V. (2018). Isolating the liquid cloud response to recent Arctic sea ice variability using spaceborne lidar observations. *Journal of Geophysical Research: Atmospheres*, *123*, 473–490. https://doi.org/10.1002/2017JD027248

Received 5 JUN 2017
Accepted 4 DEC 2017
Published online 10 JAN 2018

Isolating the Liquid Cloud Response to Recent Arctic Sea Ice Variability Using Spaceborne Lidar Observations

A. L. Morrison[1,2], J. E. Kay[1,2], H. Chepfer[3], R. Guzman[4], and V. Yettella[1,2]

[1]Department of Atmospheric and Oceanic Sciences, University of Colorado Boulder, Boulder, CO, USA, [2]Cooperative Institute for Research in Environmental Sciences, University of Colorado Boulder, Boulder, CO, USA, [3]Laboratoire de Météorologie Dynamique, IPSL, Université Pierre et Marie Curie, Paris, France, [4]Laboratoire de Météorologie Dynamique, IPSL, Centre National de la Recherche Scientifique, Ecole Polytechnique, Palaiseau, France

Abstract While the radiative influence of clouds on Arctic sea ice is known, the influence of sea ice cover on Arctic clouds is challenging to detect, separate from atmospheric circulation, and attribute to human activities. Providing observational constraints on the two-way relationship between sea ice cover and Arctic clouds is important for predicting the rate of future sea ice loss. Here we use 8 years of CALIPSO (Cloud-Aerosol Lidar and Infrared Pathfinder Satellite Observations) spaceborne lidar observations from 2008 to 2015 to analyze Arctic cloud profiles over sea ice and over open water. Using a novel surface mask to restrict our analysis to where sea ice concentration varies, we isolate the influence of sea ice cover on Arctic Ocean clouds. The study focuses on clouds containing liquid water because liquid-containing clouds are the most important cloud type for radiative fluxes and therefore for sea ice melt and growth. Summer is the only season with no observed cloud response to sea ice cover variability: liquid cloud profiles are nearly identical over sea ice and over open water. These results suggest that shortwave summer cloud feedbacks do not slow long-term summer sea ice loss. In contrast, more liquid clouds are observed over open water than over sea ice in the winter, spring, and fall in the 8 year mean and in each individual year. Observed fall sea ice loss cannot be explained by natural variability alone, which suggests that observed increases in fall Arctic cloud cover over newly open water are linked to human activities.

1. Introduction

Arctic sea ice loss since 1979 (Screen & Simmonds, 2010; Serreze et al., 2009; Stroeve et al., 2012) is one of the most visible manifestations of recent human-caused (Bindoff et al., 2013; Kay et al., 2011; Kirchmeier-Young et al., 2017; Min et al., 2008) climate change. Clouds can respond to sea ice loss by forming over newly open water, but this potential is not a given. Understanding the cloud response to sea ice loss is important because cloud changes can accelerate or decelerate future sea ice loss. Present-day climatologies show the substantial influence of Arctic clouds on sea ice melt and growth over the seasonal cycle (Curry et al., 1993; Intrieri, Fairall, et al., 2002; Kay & L'Ecuyer, 2013; Shupe & Intrieri, 2004). During summer when shortwave cloud radiative effects dominate over longwave cloud radiative effects, Arctic clouds cool the surface and reduce sea ice melt. In all other seasons, longwave cloud radiative effects dominate and Arctic clouds warm the surface. Increasing summer clouds would replace one bright surface (lost sea ice) with another (new clouds) and decelerate future sea ice loss. Increasing clouds in all other seasons would warm the surface even more and accelerate future sea ice loss (e.g., Abbot & Tziperman, 2009). Clouds containing liquid water (hereafter "liquid clouds"), especially near-surface liquid clouds below 3 km, contribute more strongly to cloud-induced surface warming and cooling than ice-only clouds (Bitz et al., 2005; Matus & L'Ecuyer, 2017; Morrison et al., 2012; Sedlar et al., 2011; Shupe & Intrieri, 2004). Atmospheric temperature alone is not predictive of cloud phase: liquid clouds occur in all seasons, at temperatures as low as −40°C, and often persist for several days (Cesana et al., 2012; Intrieri, Shupe, et al., 2002; Morrison et al., 2012; Shupe et al., 2006; Verlinde et al., 2007).

Air-sea coupling affects low cloud formation and maintenance and thus is important to consider when introducing the potential for a cloud response to sea ice loss. When the ocean and lower atmosphere are coupled, as they are over much of the world's oceans, moisture transfer from the open water to the lower atmosphere promotes low cloud formation (Klein & Hartmann, 1993). The Arctic atmosphere can be coupled or decoupled from the ocean. Whether the Arctic atmosphere and sea surface are coupled depends in part

on Arctic cloud properties such as cloud altitude and the strength of cloud-forced vertical mixing (Morrison et al., 2012; Shupe et al., 2013). Air-sea coupling also depends in part on air-sea temperature gradients, which, in turn, are affected by (1) the seasonal cycle of solar radiation and (2) the higher specific heat capacity of water compared to air. These two factors lead to the assumption of a seasonal difference in air-sea temperature gradients and therefore in the air-sea coupling that drives Arctic cloud responses to sea ice loss. Near-surface static stability is a measure of air-sea coupling strength (Klein & Hartmann, 1993) and is one of the most important indicators of a cloud response to sea ice loss (Kay & Gettelman, 2009). In summary, seasonal differences in air-sea coupling lead us to hypothesize both the absence of a summer cloud response and the presence of fall cloud response (hereafter referred to as the "local air-sea coupling hypothesis").

The goal of this study is to isolate the observed influence of Arctic sea ice cover on liquid cloud profiles. Building on previous research, we recognize that accurately isolating the influence of sea ice cover on clouds requires four elements: (1) a seasonal approach, (2) active satellite observations, (3) a local and instantaneous perspective, and (4) using a novel isolation method that separate the influence of sea ice cover on clouds from other cloud-controlling factors (e.g., atmospheric circulation). First, separating the analysis by season is required by the governing physics. Some previous studies (e.g., Barton et al., 2012; Liu et al., 2012) overlooked the need for seasonal separation. Studies indicate that summer Arctic clouds do not respond to summer sea ice loss (Kay & Gettelman, 2009) but that more fall clouds form over open water than over sea ice (Kay & Gettelman, 2009; Palm et al., 2010; Sato et al., 2012; Schweiger et al., 2008; Wu & Lee, 2012). Second, this analysis requires observational tools that provide accurate cloud detection independent of the underlying surface type. Available over the last decade only, spaceborne active sensors (Chepfer et al., 2010; Winker et al., 2010) provide surface-blind cloud profiling from 82°S to 82°N. Third, isolating cloud changes due to sea ice loss from other cloud-controlling factors also requires analyzing clouds at the spatial and temporal scales on which clouds and sea ice change. Previous studies (e.g., Kay et al., 2008; Kay & Gettelman, 2009; Liu et al., 2012; Palm et al., 2010; Sato et al., 2012; Schweiger et al., 2008; Wu & Lee, 2012) have generally used monthly mean gridded cloud and sea ice data. Because clouds change on sub-daily and kilometer scales, observations at the satellite footprint help extract process relationships between sea ice, clouds, and atmospheric circulation (e.g., Taylor et al., 2015). Finally, the cloud response to sea ice loss must be isolated from other cloud-controlling factors such as the large-scale atmospheric circulation. One strategy to address this concern is to define regimes based on the physical properties of the Arctic climate system. For example, Barton et al. (2012) and Taylor et al. (2015) analyzed cloud and sea ice covariance within regimes defined by lower-tropospheric stability and vertical velocity. Separating by synoptic regime has proven useful because clouds are affected by both atmospheric circulation and stability. But this method has limitations for identifying the cloud response to sea ice cover because Arctic atmospheric stability and sea ice cover can be correlated. As a result, when sea ice turns into open water, the lower-tropospheric stability regime can change. For example, observations indicate lower stability over open water than over sea ice (e.g., recent field mission described in Sotiropoulou et al. (2016)). As a consequence, when analyzing the cloud response to sea ice loss, the stability regime must be allowed to change. Stability cannot evolve with sea ice cover within controlled stability regimes. Barton et al. (2012) and Taylor et al. (2015) provide important results on cloud-sea ice relationships when synoptic (and stability) conditions are held constant; however, a key difference between those studies and the one presented here is that we are identifying a cloud response to sea ice cover without making assumptions about stability. When looking at how clouds change with sea ice cover, compositing by a property that also changes with sea ice cover (i.e., stability) may weaken the desired signal.

Building on insights gained from previous studies (Barton et al., 2012; Kay et al., 2008; Kay & Gettelman, 2009; Liu et al., 2012; Palm et al., 2010; Sato et al., 2012; Schweiger et al., 2008; Taylor et al., 2015; Wu & Lee, 2012), we analyze cloud-sea ice relationships at a local and instantaneous scale during all four seasons. We use a novel isolation method based on sea ice concentration. Our study focuses on 2008–2015, a period with large interannual variability in seasonal sea ice concentrations. Due to shrinking sea ice cover since 1979 (Serreze et al., 2009), there is enough Arctic sea ice variability over these recent 8 years to observe clouds both over sea ice and over open water. The years 2008–2015 are also a period over which the large variations in sea ice cover exist partly because of long-term human-caused sea ice loss (Bindoff et al., 2013; Kay et al., 2011; Kirchmeier-Young et al., 2017; Min et al., 2008). We want to isolate the cloud response to this observed variability in sea ice cover.

2. Data

Our study focuses on Arctic cloud and sea ice relationships during summer (June–August) and fall (September–November) over the period 2008–2015. We are limited to this 8 year period because we use first-in-kind cloud observations from the spaceborne Cloud-Aerosol Lidar with Orthogonal Polarization (CALIOP) lidar on board the Cloud-Aerosol Lidar and Infrared Pathfinder Satellite Observation (CALIPSO) satellite. Though CALIPSO was launched in 2006, we only use cloud data starting in 2008 because the satellite tilt changed in November 2007. CALIPSO's geographical range spans from 82°S to 82°N. As an active sensor, CALIPSO has unique strengths in detecting thin clouds, cloud layers, cloud phase, and clouds over sea ice. Importantly, the CALIPSO lidar measures cloud vertical structure and phase independent of surface conditions and temperature assumptions. One limitation of the CALIPSO lidar is that the measured signal is attenuated by optically thick clouds (Chepfer et al., 2010; Winker et al., 2010); however, since clouds in the Arctic are often optically thin, the penetration depth of the lidar is often close to the surface. In this study, we will quantitatively examine the profiling capabilities of CALIPSO in the Arctic, building on the work of Guzman et al. (2017).

For this study, we used an established CALIPSO product: the CALIPSO-GCM-Oriented CALIPSO Cloud Product (CALIPSO-GOCCP), version 3.0 (Cesana & Chepfer, 2013; Chepfer et al., 2010, 2013; Guzman et al., 2017). Briefly, GOCCP is developed from Level 1 version 3.30 CALIOP data. The CALIOP 532 nm Attenuated Backscatter profile and Goddard Modeling and Assimilation Office Molecular Density profiles are used to calculate a vertical lidar scattering ratio (SR) profile but are first processed onto a vertical grid with vertical resolution of 480 m to ensure uniform vertical resolution (Chepfer et al., 2010). SR thresholds then separate an atmospheric layer into clouds, clear sky, unclassified, or fully attenuated by opaque clouds. Below 8 km, the GOCCP data product provides clouds' horizontal and vertical locations at 333 m horizontal and 480 m vertical resolutions. If a cloud is detected, the attenuated total backscatter and cross-polarized total attenuated backscatter are used to determine cloud phase (Cesana & Chepfer, 2013). If it is determined that a cloud contains liquid, that cloud is classified as "liquid-containing" because the "mixed-phase" classification is not used in GOCCP. The GOCCP data set has been validated in the Arctic against ground-based observations (Lacour et al., 2017), aircraft observations (Cesana et al., 2016), and other satellite cloud climatologies (Chepfer et al., 2010; Chepfer et al., 2013; Cesana et al., 2016). GOCCP was also part of the GEWEX Cloud Assessment Exercise (Stubenrauch et al., 2013).

Each CALIPSO Level 1 satellite footprint includes a sea ice concentration value, which is incorporated into the GOCCP product. Sea ice observations are from the National Snow and Ice Data Center's Near Real-Time SSM/I EASE Grid Daily Global Sea Ice Concentration and Snow Extent data product (Nolin et al., 1998). The daily sea ice concentration observations are provided at a 25 km horizontal resolution from passive microwave imagery. Each day, every cloud profile along each orbit track receives the sea ice concentration value that corresponds to the closest latitude/longitude of that particular satellite footprint. Compared to regional Canadian sea ice charts, the uncertainty in satellite-derived Arctic sea ice concentration measurements ranges from ±5% in winter to ±15% in the summer (Agnew & Howell, 2003).

A reanalysis product—the European Center for Medium-Range Weather Forecasts' ERA-Interim (Dee et al., 2011)—was used to assess atmospheric conditions during the study period. Specifically, we used 6-hourly ERA-Interim temperature profile and sea level pressure values calculated at a 0.125° × 0.125° horizontal resolution. ERA-Interim is initialized with daily passive microwave SSM/I sea ice concentration data (Breivik et al., 2001), which is the same instrument and temporal resolution as CALIPSO's sea ice data. We only use ERA-Interim when pan-Arctic near-instantaneous observations have large uncertainties or are not available, which is the case for Arctic air temperature profiles and sea level pressure. Compared to observed temperatures from Atmospheric Infrared Sounder satellite retrievals, ERA-Interim temperature biases against Integrated Global Radiosonde Archive measurements are smaller and less affected by cloud properties (Wong et al., 2015). Pressure is generally well represented in ERA-Interim when compared to atmospheric measurements from ship cruises (de Boer et al., 2014). We mapped sea level pressure and near-surface static stability values from ERA-Interim onto the satellite footprint to assess the atmospheric conditions coincident with cloud observations.

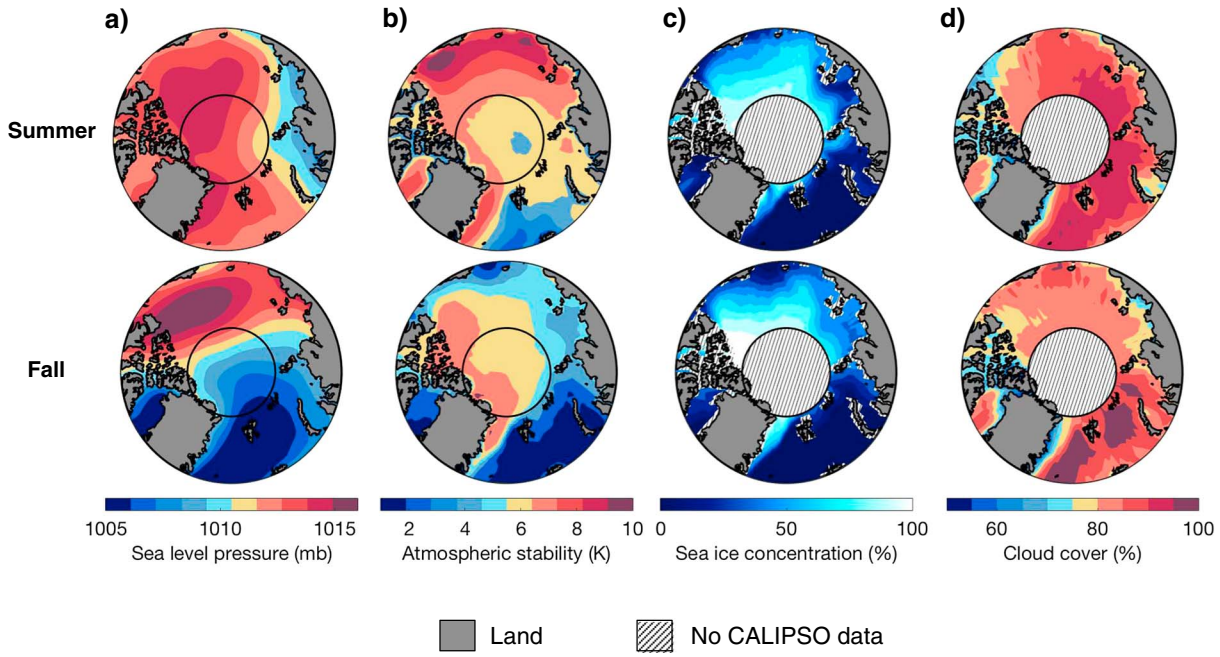

Figure 1. Seasonal mean Arctic Ocean maps of (a) sea level pressure, (b) near-surface static stability (difference between the potential temperature at 925 mb and the potential temperature at 1,000 mb ($\Theta_{925mb} - \Theta_{1000mb}$) (Kay & Gettelman, 2009)), (c) sea ice concentration, and (d) total CALIPSO-GOCCP cloud cover. The circle at 82°N is the northernmost extent of CALIPSO observations. Sea level pressure and stability data are from ERA-Interim. Sea ice concentration and cloud cover are from CALIPSO-GOCCP. Data used are gridded monthly means from 2008 to 2015.

3. Methods

3.1. Identifying the Analysis Region: The Intermittent and Perennial Masks

The Arctic is often defined as the area poleward of 70°N. But within this region there are large geographic variations in atmospheric circulation, near-surface static stability, sea ice concentration, and cloud fraction (Figure 1). We want to focus our analysis on the region of the Arctic where sea ice concentration has varied during our study period. To identify this region, we used daily sea ice concentration observations (Nolin et al., 1998) gridded into a $1° \times 1°$ grid to develop two surface masks: the perennial mask and the intermittent mask.

The first surface mask—the perennial mask—isolates regions of the Arctic Ocean where the daily sea ice concentration is invariant from 2008 to 2015. All data within the perennial mask are excluded from our analysis. Specifically, the perennial mask contains grid boxes that were always ice-free (sea ice concentration $< 15\%$; Fetterer et al., 2002), always ice-covered (sea ice concentration $> 80\%$; Strong & Rigor, 2013), or land. In this case "always" means that the daily mean sea ice concentration in a grid box was either $<15\%$ or $>80\%$ every day in a given season from 2008 to 2015. Sea ice concentrations are not provided for coastal pixels due to greater retrieval uncertainty near land, so coastal pixels are also included in the perennial mask.

The second surface mask—the intermittent mask—contains all grid boxes that are not in the perennial mask. In other words, the intermittent mask isolates regions of the Arctic Ocean where the daily sea ice concentration varies from 2008 to 2015. All data within the intermittent mask are included in our analysis. Specifically, the intermittent mask contains grid boxes that never remain only ice-free (daily sea ice concentration $< 15\%$) or only ice-covered (daily sea ice concentration $> 80\%$).

The purpose of using the intermittent mask is twofold. First, our sole focus on local instantaneous data within the intermittent mask enables us to isolate the cloud response to sea ice variations. One might be tempted to connect gridded monthly mean cloud cover with gridded monthly mean sea ice. By ignoring the need to work at a near-instantaneous time scale, this analysis strategy risks contaminating the intended signal (cloud response to sea ice loss) with noise (e.g., cloud response to atmospheric circulation variability). In addition to using a perspective that is instantaneous in time, one must also use a local perspective. For instance, analyzing clouds in a pan-Arctic perspective across the entire Arctic Ocean would compare cloud formation in the

North Atlantic and in the Beaufort Sea, two regions with very different atmospheric conditions (Figures 1a and 1b). Averaging clouds over the North Atlantic with clouds over the Beaufort Sea will not show liquid clouds' response to sea ice loss. Instead, it will show the geographic variations in clouds associated largely with differing large-scale circulation patterns. Analyzing mean cloud profiles over the entire Arctic Ocean would also lead to the erroneous conclusion that there are always more clouds over open water than over sea ice because the North Atlantic is seasonally ice-free (Figure 1c) and has a seasonal mean cloud fraction >80% (Figure 1d). Naturally, averaging cloud profiles over the North Atlantic will show more clouds over open water than over sea ice. But the North Atlantic is always ice-free for reasons unrelated to sea ice loss (Serreze et al., 1997). Therefore, the cloud response to sea ice loss cannot be observed in the North Atlantic. Similarly, the instantaneous cloud response to sea ice loss cannot be isolated in regions where sea ice cover is not changing, whether the ocean is always ice-free or always ice-covered. Any areas where sea ice concentration is invariant (i.e., those in the perennial mask) need to be excluded from this study.

3.2. Calculating the Vertical Liquid Cloud Fraction Over Sea Ice and Over Open Water

Our end goal was to compare climatological liquid cloud profiles over sea ice and over open water within the intermittent mask. We obtained the climatological liquid cloud profile over sea ice by examining instantaneous lidar profiles whenever the daily sea ice concentration exceeded 80%. We obtained the climatological liquid cloud profile over open water by examining instantaneous lidar profiles whenever the daily sea ice concentration was less than 15%. By focusing on the extremes within the intermittent mask (i.e., <15% and >80% sea ice concentrations), sea ice measurement uncertainty was unlikely to cause an "ice-free" to be accidentally classified as an "ice-covered" region or vice versa. Note that the separation of sea ice and open water within the intermittent mask and the definition of the intermittent mask are distinct.

Each instantaneous lidar profile within a satellite overpass contains several flags for clouds, clear sky, and uncertain lidar returns. We first gridded all the overpasses in a 1° × 1° grid, finding the total number of cloud, clear sky, and uncertain returns within each grid box for each satellite overpass. Using the number of returns at each altitude, we then calculated a daily cloud fraction over open water and over sea ice within each box. We define liquid cloud fraction profile in each 1° × 1° grid box as

$$\mathrm{LCF}(z) = \frac{N_{cl,liq}(z)}{N_{cl,tot}(z) + N_{clear}(z) + N_{uncertain}(z)} \tag{1}$$

where LCF is the liquid cloud fraction, $N_{\mathrm{cl,liq}}$ is the number of liquid cloud returns, $N_{\mathrm{cl,tot}}$ is the number of total cloud returns, N_{clear} is the number of clear sky returns, and $N_{\mathrm{uncertain}}$ is the number of uncertain returns. If a liquid cloud fraction was calculated over sea ice, then all the calculation inputs (i.e., cloud, clear sky, and uncertain returns) in equation (1) only occurred over sea ice. Likewise, if the vertical liquid cloud fraction was calculated over open water, then all the returns in equation (1) were only over open water.

The process of calculating vertical liquid cloud fraction was repeated for every overpass in each season from 2008 to 2015. Once gridded, we spatially averaged the cloud profiles across the intermittent mask. Gridded cloud profiles within the intermittent mask were first area-weighted by the cosine of their latitude. Averaging the profiles took the sampling density into account. Overpasses were only included in the cloud fraction calculation if they contained a liquid cloud over open water or over sea ice. The number of overpasses per box was recorded to ensure that each box was well-sampled. If a box received no overpasses during a given day, then the spatially averaged cloud fraction did not include that box on that day. Over the 8 year period, every grid box in the summer (fall) received at least 74 (63) overpasses that were used in the cloud fraction calculations. Due to CALIPSO's sampling density, grid boxes near the poles received more than 1,300 (1,000) overpasses in the summer (fall). On average, a grid box during summer (fall) received roughly 346 (287) overpasses.

When assessing differences between cloud profiles over open water and over sea ice, we must account for nonindependent lidar returns. CALIPSO cloud observations may be spatially correlated along the same orbit track (e.g., Liu et al., 2010; Marchand et al., 2006; Thorsen et al., 2011; van de Poll et al., 2006). To account for spatial correlations in the data, we use every separate overpass within each grid box as an independent sample in a Student's *t* test (95% confidence level). Arctic cloud properties tend to be correlated on spatial scales of ~2 km (Schafer et al., 2017; Tompkins & di Giuseppe, 2015), which is smaller than the length of a typical overpass within a 1 × 1° grid box. In total, the summer and fall *t* tests each used more than 250,000

overpasses over the 8 year period. Our goal was to see the altitudes at which cloud profiles were significantly different over sea ice and over open water. As with the cloud profiles, atmospheric variables from ERA-I were weighted and averaged across the intermittent mask to obtain mean sea level pressure and mean near-surface static stability values over sea ice and over open water.

3.3. Atmosphere Obscured by Lidar Attenuation

Spaceborne lidars like CALIPSO cannot measure atmospheric structure below opaque clouds-that is, clouds with an optical thickness greater than ~3 (Chepfer et al., 2010). Therefore, it is important to characterize the influence of lidar attenuation on Arctic cloud profiles, and in particular to assess if there are differences in lidar attenuation over sea ice and over open water. Our study is the first to do a thorough assessment of the lidar attenuation and the opaque cloud distribution in the Arctic. Following Guzman et al. (2017), a cloud is defined as "opaque" if the lidar detects a cloud but no surface return underneath. We used GOCCP's altitude of maximum opacity flag to determine the vertical location of opaque clouds (Guzman et al., 2017). The altitude of maximum opacity is the altitude of the lowest opaque cloud in the atmospheric column when there is no detected surface return. Below this altitude the atmosphere is fully attenuated. We also calculated how much of the atmospheric column is obscured by lidar attenuation by comparing the number of opaque clouds detected to the total number of lidar returns at each atmospheric level. We define the percent of atmosphere attenuated at every level as

$$PA(z) = \frac{N_{cl,opq}(z)}{N_{clear}(z) + N_{cl,tot}(z) + N_{surf} + N_{FA}(z)}. \quad (2)$$

where PA is percent of atmosphere that has been fully attenuated, $N_{\mathrm{cl,opq}}$ is the cumulative number of fully opaque clouds, N_{clear} is number of clear-sky returns, $N_{\mathrm{cl,tot}}$ is number of total cloud returns, N_{surf} is the number of surface returns, and N_{FA} is number of fully attenuated returns. If a surface return is not detected, all the returns below the lowest cloud return will be full attenuated returns. $N_{\mathrm{cl,opq}}$ is cumulative because we add the total number of $N_{\mathrm{cl,opq}}$ flags at a given altitude across the intermittent mask, and all the $N_{\mathrm{cl,opq}}$ flags higher than that altitude. If the lidar is attenuated at 960 m, for example, then no clouds will be detected below 960 m. The percent of atmosphere attenuated below 960 m must account for all $N_{\mathrm{cl,opq}}$ flags at 960 m and above that altitude as well. N_{FA} will change based on altitude because the number of fully attenuated returns depends on the number of opaque clouds in the atmospheric column. To determine if there was a difference in lidar attenuation over open water and over sea ice in any season, we separated all the lidar returns in equation (2) over open water and over sea ice.

4. Results

4.1. Absence of a Summer Cloud Response to Sea Ice Loss

Within the summertime intermittent mask (Figure 2a), the mean observed liquid cloud profiles over open water and over sea ice are nearly identical (Figure 2b). Statistically, the profiles are different at the 95% confidence level near the surface. Even though the differences are significant, however, they are quite small. Furthermore, each independent year of observations shows very small differences between cloud profiles over open water and over sea ice (Figure 3). When the cloud fraction profiles over ice were subtracted from cloud fraction profiles over water, the difference in every year is within 6% of zero for the entire profiled atmospheric column. Taken together, the results shown in Figures 2 and 3 provide no evidence for a summer cloud response to summer sea ice loss.

Consistent with the absence of a cloud response in summer, we found the ERA-Interim near-surface static stabilities over open water cloud profiles (5.9 ± 0.4 K) and over sea ice cloud profiles (5.5 ± 0.4 K) are very similar. The ERA-Interim average sea level pressure is also similar over open ocean cloud profiles (1,012 ± 2 mb) and sea ice cloud profiles (1,014 ± 4 mb) during summer, providing evidence that surface-dependent circulation biases do not contaminate the results shown in Figures 2 and 3. In other words, we have successfully averaged over many different circulation regimes within the intermittent mask to isolate the influence of surface conditions on clouds.

Is there an overall relationship between the mean summertime sea ice concentration and vertical cloud fraction within the intermittent mask? In other words, are years with the lowest mean sea ice concentration from 2008 to 2015 more likely to be the cloudiest years? Or are years with the lowest mean sea ice concentration

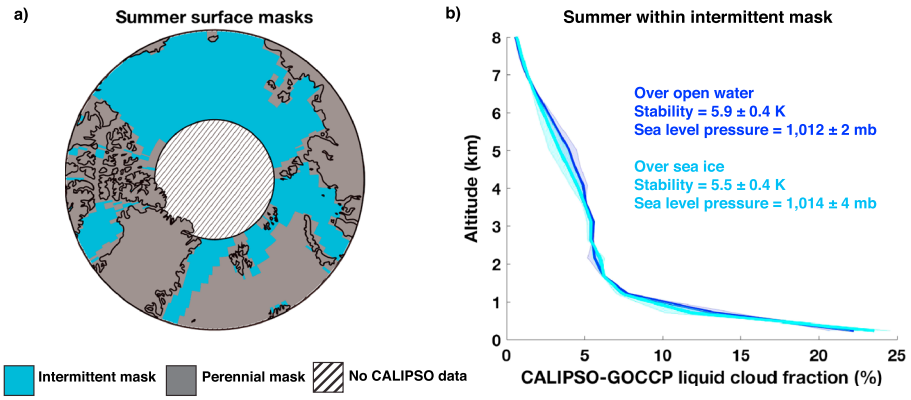

Figure 2. Observed summer liquid cloud response to recent Arctic sea ice variability: (a) the intermittent and perennial masks and (b) liquid cloud profiles over open water and over sea ice within the intermittent mask. The perennial mask includes pixels that are always sea ice-covered, always open water, or always land in every year from 2008 to 2015. The intermittent mask includes all other pixels or pixels where sea ice concentration varies from year to year. Instantaneous cloud profiles are only used within the intermittent mask and if they occur over sea ice concentrations less than 15% ("over open water") or greater than 80% ("over sea ice"). The climatological means over open water and over sea ice are the thick dark blue and light blue lines, respectively. The purple and light blue shaded regions are the 95% confidence intervals around the mean cloud profile over open water and over sea ice, respectively. During summer, over open water within the intermittent mask, the mean near-surface static stability is 5.9 K and the mean sea level pressure is 1,012 mb. Over sea ice within the intermittent mask the mean summertime near-surface static stability is 5.5 K and the mean sea level pressure is 1,014 mb.

more likely to be the least cloudy years? As expected based on the similar summer cloud profiles over open water and sea ice (Figures 2 and 3), we find no overall pattern between the mean sea ice concentration in a given year and the clouds in that year (Figure 4). Figure 4 is shown for qualitative interpretation and is not meant to isolate the influence of sea ice on clouds. We have shown that averaging over open water and sea ice profiles within the intermittent mask is a better tool for this purpose. Instead, Figure 4 highlights that sea ice variability is not a first-order control on year-to-year summer cloud variability when averaged over the entire intermittent mask.

The source regions for the summer liquid cloud profiles over open water and over sea ice are shown in Figure 5. In total, over 60% of all observed liquid cloud profiles from 2008 to 2015 within the intermittent mask were used. The mean profile over open water (sea ice) uses 35% (26%) of all the instantaneous cloud profiles within the intermittent mask. The profiles over open water are mostly located around the margins of the intermittent mask (Figure 5a). The observed liquid cloud profiles over sea ice are mostly located in the center of the intermittent mask (Figure 5b).

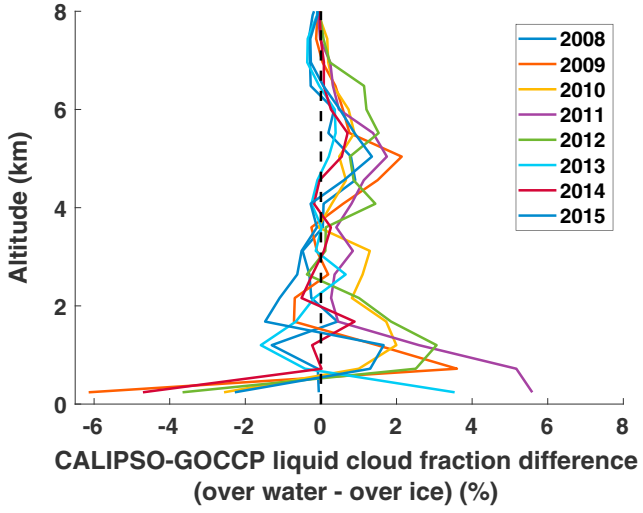

Figure 3. The difference between vertical liquid cloud fraction over water and over ice for every year from 2008 to 2015 during summer.

4.2. Detection of a Fall Cloud Response to Sea Ice Loss

In contrast to the summer (Figure 2), the results from the intermittent mask during fall (Figure 6a) indicate more liquid clouds over open water than over sea ice (Figure 6b). In other words, we do find evidence for an observed fall liquid cloud response to sea ice loss. Based on the Student's *t* test (95% confidence level), there are significantly more liquid clouds over open water than over sea ice from 0.24 to 9.36 km. The altitude range values are the midpoints of each altitude bin where the difference between cloud fraction over water and over sea ice was statistically significant. Compared to the summer, the differences in fall cloud profiles are both significant and large, indicating that the cloud fraction differences in the fall are physically meaningful. On average, below 8 km the mean cloud fraction over open water is nearly 150% of the mean cloud fraction over sea ice. A fall cloud response to sea ice loss can also be seen by looking at individual years of data. In

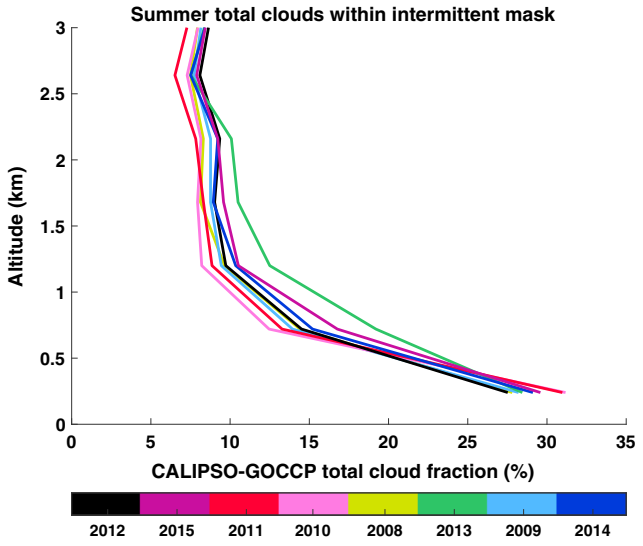

Figure 4. Summer total low cloud profiles (<3 km) ranked from lowest to highest mean sea ice concentration within the intermittent mask in each year.

every year from 2008 to 2015 the cloud fraction difference between profiles over open water and over sea ice is positive down to 240 m above the surface (Figure 7). Taken together, the results shown in Figures 6 and 7 provide strong evidence for a fall cloud response to sea ice loss.

To confirm that the larger cloud fraction over open water is a response to the surface and not to a specific synoptic regime, we compared atmospheric conditions over open water and over sea ice. Consistent with the presence of a stability-driven cloud response in fall, the ERA-Interim near-surface static stability over sea ice (4.6 ± 0.3 K) is larger than that over water (2.6 ± 0.3 K) (Figure 6b). We find small differences in ERA-Interim sea level pressure between the profiles over open water (1,009 ± 2 mb) and the profiles over sea ice (1,010 ± 3 mb). The small differences in stability and sea level pressure suggest that, similar to summer, we have successfully isolated the surface influence on clouds over many circulation regimes and surface-dependent circulation biases do not contaminate the results shown in Figures 6 and 7.

Again, is there an overall relationship between the mean fall sea ice concentration and low-level vertical cloud fraction within the intermittent mask? Unlike in summer, during fall an overall pattern between cloud fraction and sea ice cover begins to emerge when we average over individual years over the entire intermittent mask (Figure 8). The low-level vertical (below 1.5 km) cloud fractions are generally largest in low sea ice years and decrease as mean fall sea ice concentration in the intermittent mask increases. We interpret Figure 8 qualitatively, with the caveat that 8 years is a short record to see patterns between total cloud cover and total sea ice concentration. Figure 8 suggests that fall sea ice variability influences cloud variability, but it is also clear from the figure that there are other influences on Arctic clouds beyond sea ice.

As in Figure 5 for summer, the source regions for the fall liquid cloud profiles over open water and over sea ice are shown in Figure 9. Our analysis used nearly 80% of the instantaneous cloud profiles within the intermittent mask during fall (Figure 9). Specifically, the 8 year mean fall profile over open water (sea ice) uses 45%

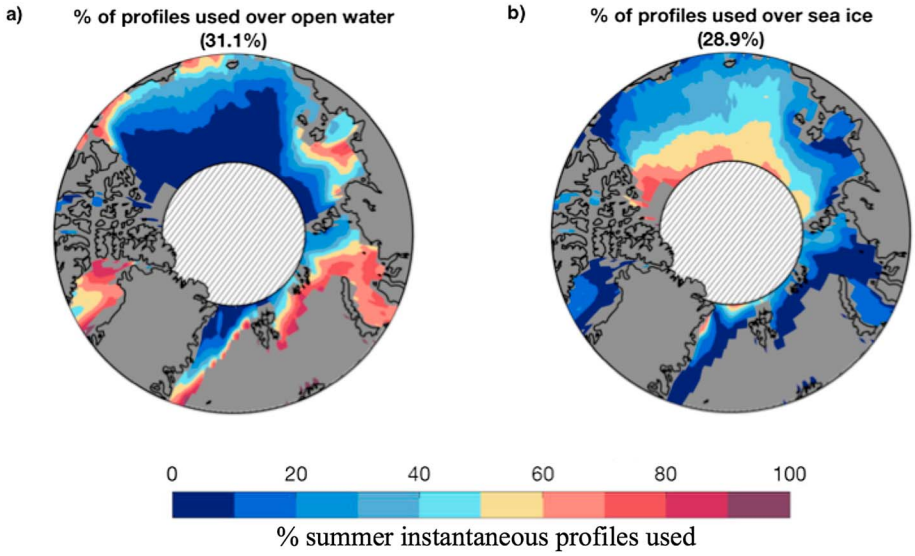

Figure 5. Percent of summer instantaneous liquid cloud profiles within the intermittent mask over (a) open water and (b) sea ice. Sea ice concentration at the satellite footprint is used to separate instantaneous cloud profiles over open water and instantaneous cloud profiles over sea ice. On average (a) 31.1% of instantaneous cloud profiles occurred over open water and (b) 28.9% of instantaneous cloud profiles occurred over sea ice.

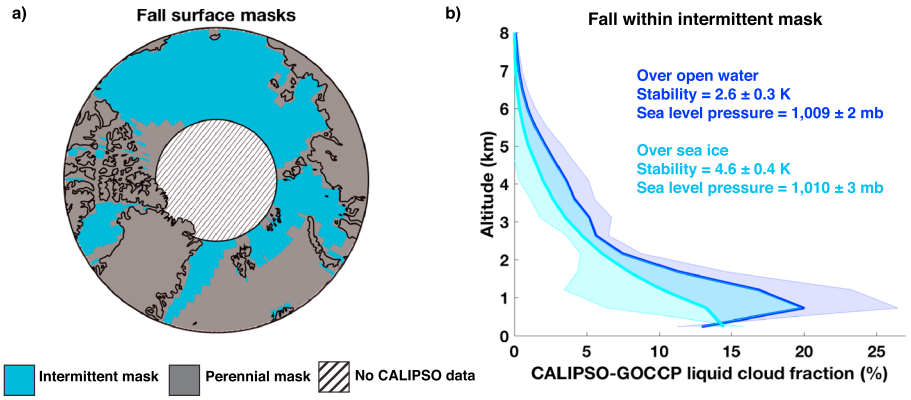

Figure 6. As in Figure 2 except for fall. Based on a Student *t* test (95% confidence level), the mean fall cloud profiles over open water and over sea ice are statistically different from 0.240 to 9.36 km. During fall, over open water within the intermittent mask, the mean near-surface static stability is 2.6 K and the mean sea level pressure is 1,009 mb. Over sea ice within the intermittent mask the mean near-surface static stability is 4.6 K and the mean sea level pressure is 1,010 mb.

(34%) of all the instantaneous cloud profiles within the intermittent mask. Only about 20% of fall instantaneous cloud profiles occurred over the marginal ice zone. While more profiles were used overall in the fall than in the summer, the location of open water and sea ice profiles is similar: fall open water profiles are also located around the margins of the intermittent mask, though there are more open water profiles near the Bering Strait and the Barents Sea in fall than in summer (Figure 9a). The sea ice profiles during fall are clustered in the Central Arctic Ocean (Figure 9b).

4.3. Influence of Geographic Subsampling on Cloud Profiles Over Sea Ice and Open Water

A useful way to test the robustness of our main summer and fall results (Figures 2 and 6) is to evaluate the sensitivity of these results to geographic subsampling within the intermittent mask. Robustness to geographic subsampling means that we expect the same results everywhere within the intermittent mask. Mainly, we wish to test the air-sea coupling hypothesis in regions with different climatological sea level pressure. The air-sea coupling physics governing the cloud response are the same across the whole Arctic, so the same signal should be observed in different subregions of the intermittent mask. In other words, our results should emerge from the local coupling physics and not because of nonlocal compensation.

We begin assessing the robustness of our results to geographic subsampling by checking summer profiles over the Beaufort Sea, 70–82°N, 156–125°W (Figure 10a). The Beaufort Sea is a revealing region because its atmospheric circulation patterns are dominated by high pressure (Figure 1a) (Serreze & Barrett, 2011). As in the entire intermittent mask, the 8 year mean cloud profiles over the Beaufort Sea are very similar over open water and over sea ice (Figure 10b). The cloud profiles over open water and over sea ice are statistically indistinguishable from 1.68 to 3.60 km. The interannual variability between cloud profiles is much greater in the Beaufort Sea than in the entire intermittent mask (Figure 10c). In some years the Beaufort Sea had very little sea ice cover (e.g., summer 2012), so there were few clouds observed over sea ice, which contributes to the noise of the year-to-year profiles.

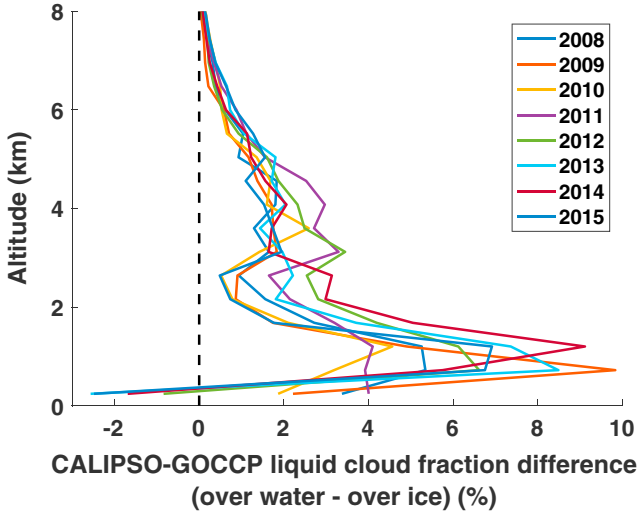

Figure 7. As in Figure 3 except for fall.

The second tested geographic subregion is the combined Barents and Kara Seas on the northern coast of Siberia, 70–82°N, 50–139°E (Figure 10d). We chose this region for several reasons. First, as shown in Figure 1a, there is a summertime sea level pressure dipole across the Arctic Ocean. The Barents and Kara Seas are the low pressure regime, where the mean summer sea level pressure is 1,010 mb. By focusing on clouds in this region, we reduce the potentially confounding effect of comparing high and low

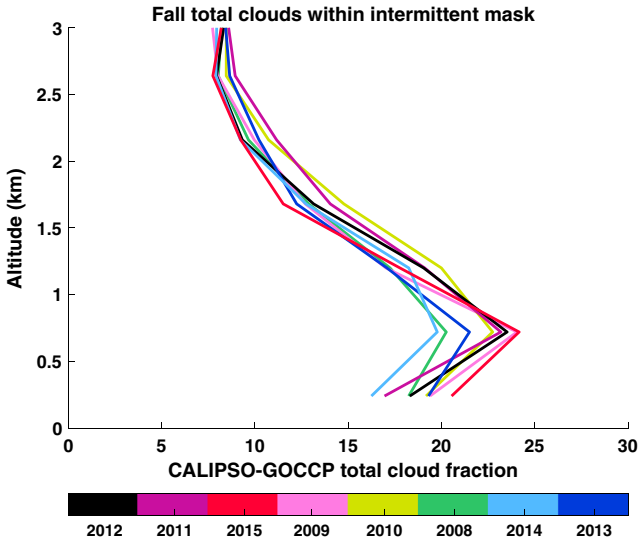

Figure 8. As in Figure 4 except for fall.

pressure regimes. Second, we can also test if there is a cloud response to sea ice loss where uplift from low pressure promotes cloud formation. Using the intermittent mask is a more elegant way to avoid comparing different synoptic regimes, but selecting regions based purely on latitude/longitude thresholds works as well. Finally, we can test the influence of geographic variability in cloud source locations. Most open water profiles come from the Barents and Kara Seas (Figure 5). Figure 10e shows that over the Barents and Kara Seas the summer cloud profiles are very similar, though there are more near-surface clouds over sea ice than over open water. There is also much less interannual variability in cloud profiles over the Barents and Kara Seas (Figure 10f) than there is over the Beaufort Sea (Figure 10c). Our summer results are robust to geographic subsampling.

For the fall, as in summer, we selected the Beaufort Sea (Figure 11a) as our first geographic subregion. The Beaufort High is stronger in the fall than it is in the summer (Serreze & Barrett, 2011), so clouds here are under a stronger subsidence region during fall than during summer. In the 8 year mean there are more liquid clouds over open water than over sea ice at every level of the atmosphere. The difference is largest below 1.5 km (Figure 11b). Except in the altitude bin from 1.92 to 2.40 km, from 0.240 to 9.36 km, the liquid cloud profile over open water is significantly larger than the liquid cloud profile over sea ice. Though the interannual profiles are noisy, generally the cloud fraction is larger over open water than over sea ice (Figure 11c). We do see the same response —more liquid clouds over open water than over sea ice—in the Beaufort Sea as in the entire intermittent mask. The magnitude of the fall response is just smaller over the Beaufort Sea. The Beaufort Sea is a good example of geographic variability within the intermittent mask; there are competing influences on clouds in this region. The Beaufort Sea is characterized by high sea level pressure and large open water extent during fall. High pressure suppresses clouds, but open water promotes cloud formation during fall. The surface conditions (i.e., sea ice versus open water) are a strong control on fall clouds. While the large-scale atmospheric circulation does not change the overall fall cloud response to sea ice cover, large-scale atmospheric circulation certainly influences Arctic cloud formation and evolution.

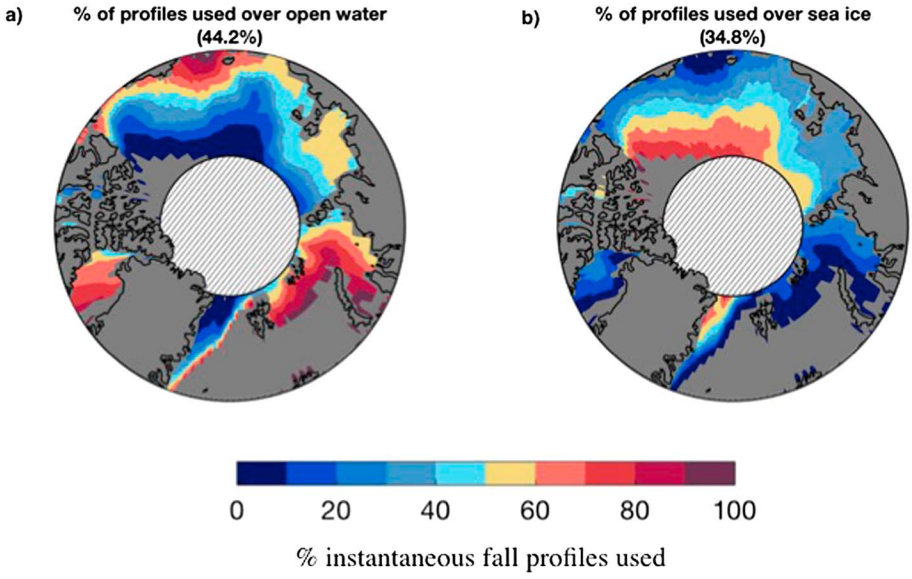

Figure 9. As in Figure 5 except for fall. On average (a) 44.2% of instantaneous liquid cloud profiles occurred over open water and (b) 34.8% of instantaneous cloud profiles occurred over sea ice.

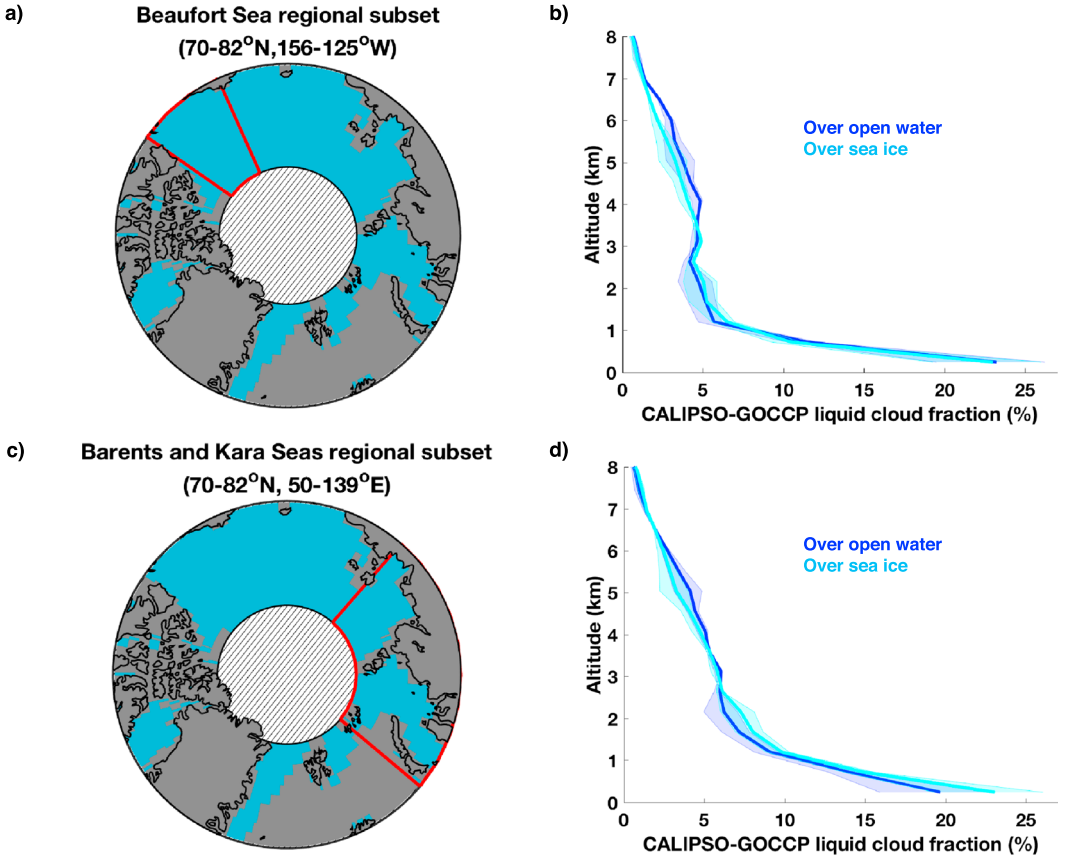

Figure 10. Robustness of summer cloud response results to regional subsetting within the intermittent mask. (a) Summer liquid cloud profiles in the Beaufort Sea (70–82°N, 125–156°W) over sea ice and open water. (b) 8 year mean summer liquid cloud profiles over open water and over sea ice in the Beaufort Sea. The purple and light blue shaded regions are the 95% confidence intervals from the mean cloud profile over open water and over sea ice, respectively. (c) Interannual variability in summer liquid cloud profiles over the Beaufort Sea. Each thin line represents the liquid cloud profile for 1 year from 2008 to 2015. (d) Summer liquid cloud profiles in the Barents and Kara Seas (70–82°N, 50–139°E) over sea ice and open water. The Barents and Kara Seas are a region dominated by low mean sea level pressure during summer (sea level pressure $<$ 1,013 mb; Figure 1a). (e) Eight-year mean summer liquid cloud profiles over open water and over sea ice in the Barents and Kara Seas. (f) Interannual variability in summer liquid cloud profiles over the Barents and Kara Seas.

The second tested geographic subregion in the fall is the combined Beaufort, Chukchi, and East Siberian Seas (BESS), 70–82°N, 270–90°E (Figure 11d). There is an atmospheric circulation dipole in the fall mean state, with the high pressure centered over the Beaufort and Chukchi Seas and the low pressure centered on the North Atlantic (Figure 1a). The intermittent mask method removes most of the clouds over the low pressure center near the North Atlantic, but not all of them. By focusing on the BESS region, we reduce the potentially confounding effect of comparing clouds in differing climatological sea level pressure regimes. The edge of the intermittent mask near the North Atlantic has climatological low sea level pressure (Figure 1a) and a large percentage of the open water profiles (Figure 9a). We must ensure that the observed fall cloud response to sea ice loss is not actually a response to the geographic collocation between open water and uplift from low pressure. In the BESS region there are more liquid clouds over open water than over sea ice in the 8 year mean (Figure 11e). The profiles are significantly different from 0.480 to 9.36 km. The overall fall cloud response to sea ice loss is the same in the BESS region as in the entire intermittent mask. The signal is much clearer in the BESS region than it is in just the Beaufort Sea: we see more liquid clouds over open water than over sea ice in every year (Figure 11f). Again, the magnitude of the signal is smaller over the BESS region than it is over the entire intermittent mask.

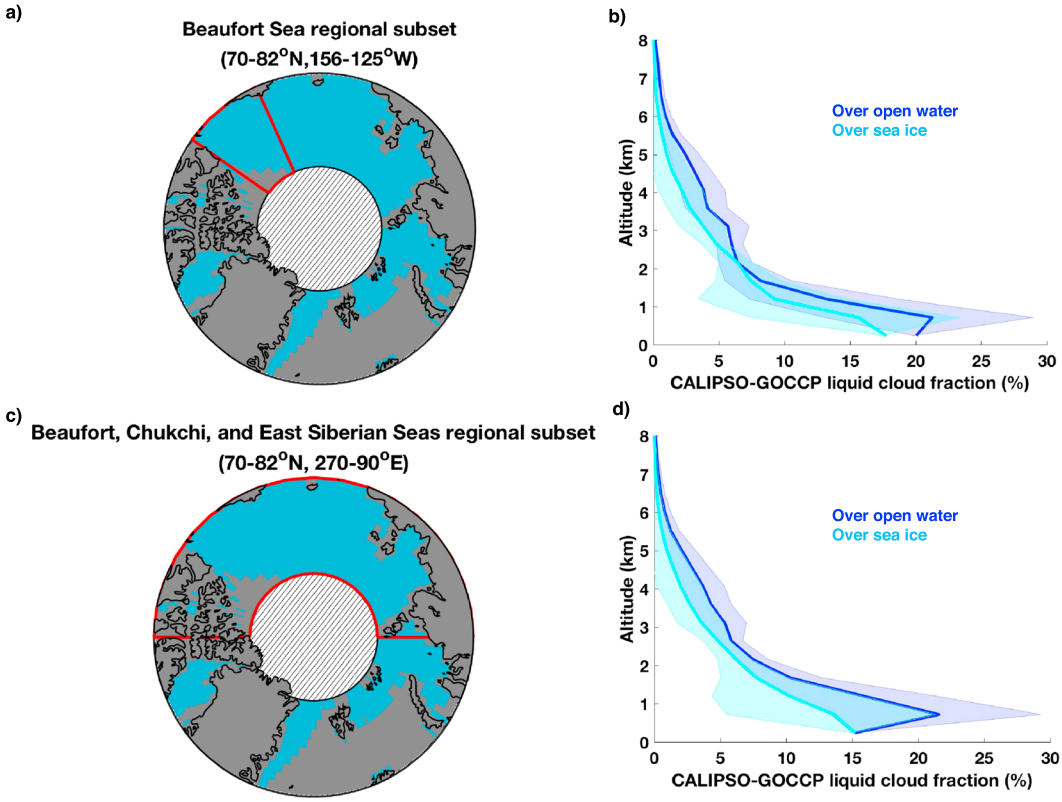

Figure 11. Robustness of fall cloud response results to regional subsetting within the intermittent mask. (a) Fall liquid cloud profiles in the Beaufort Sea (70–82°N, 125–156°W) over sea ice and open water. (b) Eight-year mean fall liquid cloud profiles over open water and over sea ice in the Beaufort Sea. The purple and light blue shaded regions are the 95% confidence intervals from the mean cloud profile over open water and over sea ice, respectively. (c) Interannual variability in fall liquid cloud profiles over the Beaufort Sea. Each thin line represents the liquid cloud profile for 1 year from 2008 to 2015. (d) Fall liquid cloud profiles in the Beaufort, Chukchi, and East Siberian Seas (70–82°N, 270–90°E) over sea ice and open water. (e) Eight-year mean fall liquid cloud profiles over open water and over sea ice in the Beaufort, Chukchi, and East Siberian Seas. (f) Interannual variability in summer liquid cloud profiles over the Beaufort, Chukchi, and East Siberian Seas.

4.4. Influence of Lidar Attenuation on Cloud Profiles Over Sea Ice and Open Water

As discussed in section 3.3, it is essential to test the robustness of our results to lidar attenuation as it passes through the atmosphere. We start with summer clouds. Using the GOCCP cloud opacity product (Guzman et al., 2017), we find that the mean summer opaque cloud cover within the intermittent mask is 53% (Figure 12a). Additionally, the mean altitude of full attenuation in the summer is 1.2 km (Figure 12b). In other words, the atmospheric column is on average fully observed down to 1.2 km. Using equation (2) we calculated the percent of atmosphere obscured by lidar full attenuation over open water and over sea ice during the summer. We found no statistically significant difference in the percentage of atmosphere fully attenuated over open water and over sea ice in the climatological mean and very little interannual variability in lidar full attenuation (Figure 12c). Returning to the Beaufort Sea, the mean opaque cloud cover is less than 30% (Figure 10a) and the mean altitude of maximum attenuation is below 1 km (Figure 12b). There is still no observed summer cloud response to sea ice loss in a region where most of the clouds are being observed. We conclude that attenuation does not invalidate our summer results (Figure 2b).

Next, we assess the impact of lidar attenuation on fall cloud profiles. There are fewer opaque clouds in the fall (Figure 13a) than in the summer (Figure 12a) (42% versus 53%, respectively). The atmospheric column is fully observed, on average, down to 0.8 km (Figure 13b), indicating that the lidar sees closer to the surface in fall than in summer. Unlike the summer, we do find evidence for a difference in lidar attenuation over open water and over sea ice during fall. In the fall, the opaque clouds occur preferentially over open water. The maps of open water profiles (Figure 9a) and of opaque cloud cover (Figure 13a) look nearly identical. If lidar attenuation through opaque clouds occurred during the fall, the majority of the time, it occurred over open water.

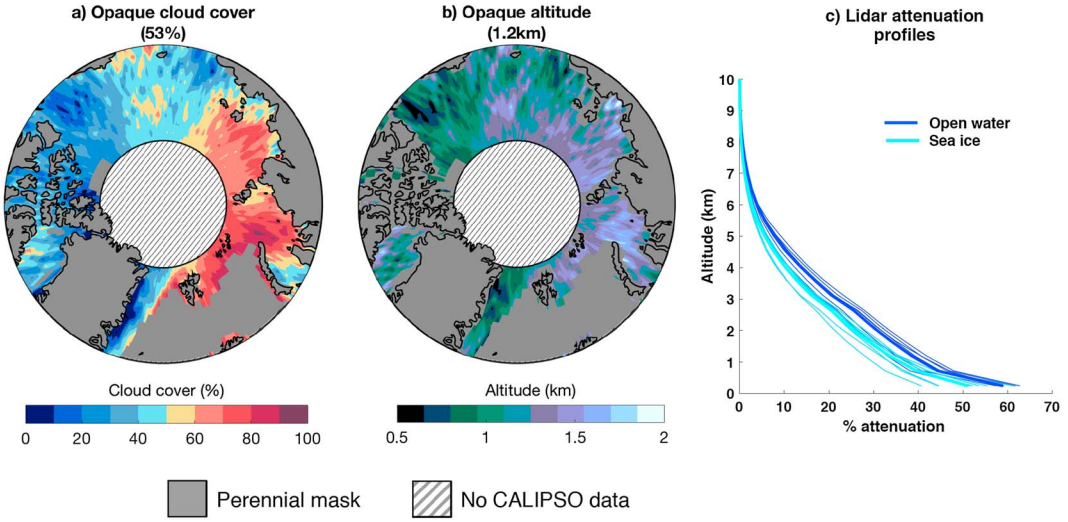

Figure 12. Maps of mean summer (a) opaque clouds, (b) altitude of maxium cloud opacity, and (c) perecent of atmosphere obscured by lidar attenuation within the intermittent mask. Data used are from 2008 to 2015. CALIPSO-GOCCP defines a cloud as "opaque" when the lidar detects a cloud but no surface return. The opaque altitude is the lowest altitude at which the lidar detects a cloud in an "opaque cloud" profile. The mean opaque cloud cover within the intermittent mask is 53%; the mean cloud opacity altitude is 1.2 km. There is no significant difference in summer lidar attenuation over open water and over sea ice.

The percent of the atmosphere fully attenuated over open water is almost equal in the summer and the fall (59% and 58%, respectively). Much less of the atmosphere is fully attenuated over sea ice in the fall than in the summer, however. Close to the surface (<2 km) during fall, the percent of atmosphere obscured by lidar attenuation over open water is twice as large as the percent of atmosphere obscured over sea ice. Below 5 km, in every year, the percent of atmosphere obscured over open water is larger than the percent of atmosphere obscured over sea ice (Figure 13c). Therefore, attenuation could be strongly impacting the fall result: more clouds are being missed over open water than over sea ice. Notably, this attenuation difference does not invalidate the fall result. It is clear that missing more clouds over open water than over sea ice would increase the separation between the open water profiles and sea ice

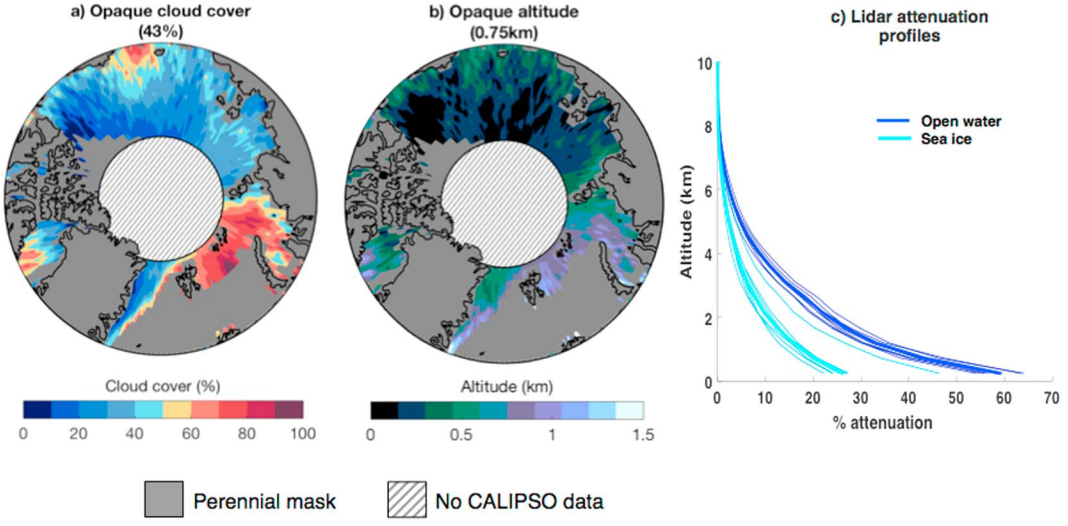

Figure 13. As in Figure 12 except for fall. During fall the mean opaque cloud cover is 43%; the mean cloud opacity altitude is 0.75 km. From 6 km to the surface, the lidar is attenuated through a larger percentage of the atmosphere over open water than over sea ice.

profiles. We now have the specific limitations from lidar attenuation: we know how much of the atmosphere is attenuated over open water and over sea ice. During fall, cloud fraction is clearly larger over open water than over sea ice, but lidar attenuation is clearly also stronger over open water than over sea ice. The main limit in the fall is that we are unable to quantify the exact magnitude of liquid cloud increase over open water because of attenuation. But we do know the range of possible cloud fraction increase: the maximum observed fall cloud fraction over water is ~20% (Figure 6b), and the largest possible fall cloud fraction over water is 20 + 58% close to the surface, where 58% is the maximum fully attenuated percent of atmosphere (Figure 13c).

5. Discussion

Our summer and fall results fit with physical understanding of the Arctic climate system. Both the lack of summer cloud response and the presence of a fall cloud response to Arctic sea ice loss can be attributed to local air-sea coupling strength and turbulent heat fluxes from the ocean to the atmosphere. Observations are needed to analyze turbulent fluxes across the Arctic Ocean (e.g., Boisvert et al., 2015; Boisvert & Stroeve, 2015; Ganeshan & Wu, 2016; Sotiropoulou et al., 2016). While heat flux observations are still difficult to obtain in the Arctic, most recent observational studies support the air-sea coupling hypothesis. Furthermore, the air-sea coupling hypothesis makes physical sense in the Arctic. During summer, the atmosphere warms from solar radiation while the ocean surface remains close to the melting temperature (Persson, 2012; Rayner et al., 2003; Tjernström et al., 2015). As a result, the summer has weak air-sea coupling (relatively warm atmosphere underlain by a cooler ocean). Moisture fluxes from the Arctic Ocean to the atmosphere during summer are small. During the summer the Arctic atmosphere and ocean are weakly coupled, as evidenced by recent field (Sotiropoulou et al., 2016) and satellite (Boisvert et al., 2015; Boisvert & Stroeve, 2015) observations. Furthermore, our results show a very small difference in ERA-I near-surface static stability over sea ice and over open water. Synoptic processes are an important influence on clouds year-round, but since summer clouds show no response to surface forcing, the dominant control on Arctic summer clouds is large-scale atmospheric circulation.

During fall, the atmosphere and ocean are more strongly coupled than they are during summer. Incoming solar radiation declines as the Sun sets, but the ocean remains relatively warm and the atmosphere cools. Observations have shown that the near-surface atmosphere is almost always at saturation over open water during fall, because the ocean is warmer than the atmosphere (Andreas et al., 2002). Importantly for cloud formation, across the entire intermittent mask, latent heat and moisture fluxes have been increasing over newly open water during the late fall (e.g., Boisvert et al., 2015; Boisvert & Stroeve, 2015). Increasing moisture fluxes have been linked to decreasing sea ice extent and a destabilized lower atmosphere (Boisvert et al., 2015). While both sensible and latent heat fluxes affect clouds, a warmer and wetter Arctic during fall may have a stronger impact on low-cloud formation than merely a warmer Arctic. The seasonal shift in air-sea coupling strength can also be seen in the difference between near-surface static stability over open water and over sea ice between the summer and fall: the stability of the fall atmosphere over sea ice is nearly twice as large as the stability of the fall atmosphere over open water. Increased air-sea coupling with more open water during fall is consistent with a deeper atmospheric boundary layer, and the CALIPSO cloud fraction profiles do indicate a deeper boundary layer over open water than over sea ice (Figure 6b). We provide observational evidence for relationships between fall clouds and sea ice.

One part of the cloud-sea ice relationship is that enhanced moisture and latent heat fluxes from newly open ocean to the atmosphere promote cloud formation over open water during fall. Another part of the cloud-sea ice relationship is that clouds also increase the likelihood of open water by hindering ice freezeup. If fall clouds formed initially in response to large-scale circulation, independent of the surface, could the clouds destabilize the boundary layer enough to create open water? In other words, what causality do we see when we observe more clouds over open water than over sea ice? We find that a larger liquid cloud fraction over open water than over sea ice is the cloud response to sea ice loss. Fall clouds over open water are associated with the same atmospheric circulation regime statistics as fall clouds over sea ice. The similarity in the sea level pressure over open water and over sea ice rules out the direction of causality from the atmosphere to the surface and supports the air-sea coupling hypothesis. Fall clouds are certainly affected by

large-scale circulation, but the results shown here are the cloud response to surface forcing and not the cloud response to atmospheric circulation forcing. Our results agree with a recent review paper (Kay et al., 2016) and with multiple studies (Kay & Gettelman, 2009; Palm et al., 2010; Sato et al., 2012; Schweiger et al., 2008; Wu & Lee, 2012), but this study uses a novel mask method to separate the observed summer and fall cloud responses to sea ice cover variability from the influence of large-scale atmospheric circulation.

Moving forward, we expect cloudier fall seasons as sea ice loss continues. Observed fall sea ice loss since 1979 and extreme events such as the record-low sea ice concentrations in September 2012 cannot be explained by modeled natural variability alone (Min et al., 2008; Bindoff et al., 2013; Kay et al., 2011; Kirchmeier-Young et al., 2017). In other words, the observed fall sea ice loss is in part caused by humans. By identifying the fall Arctic cloud response to this human-influenced sea ice loss, we build upon previous work analyzing human-caused cloud changes (Norris et al., 2016) and make another link between human activities and changes in cloud cover.

An obvious follow-on question is as follows: What about winter and spring? We provide initial results for winter and spring in the supporting information. We expect more clouds over open water than over sea ice during winter and spring due to strong air-sea coupling. This is indeed what we observe. The difference in near-surface static stability over open water and over sea ice is largest in the winter, leading to the strongest coupling of any season. We emphasize that the winter and spring results are less conclusive because the intermittent masks in winter and spring cover a much smaller area than they do in the summer and fall. Indeed, our winter and spring intermittent masks each include less than 35% of the total area of the Arctic Ocean from 70°N to 82°N. If sea ice loss becomes more pronounced, the intermittent mask will include more data in the winter and spring and these initial results should be revisited.

Many studies have recognized the first-order importance of clouds to the future climate trajectory (Bony et al., 2015; Dufresne & Bony, 2008; Webb et al., 2013). Isolating the influence of sea ice on clouds has important implications for Arctic climate feedbacks. Observations suggest that summer shortwave cloud feedbacks do not slow Arctic sea ice loss. First, there is no evidence that summer cloud fraction will increase in response to changes in sea ice cover. Since clouds do not form over newly open ocean in summer, one shrinking reflective surface (sea ice) is not being replaced by another (new clouds). As a consequence, sea ice loss leads to increased absorption of solar radiation. Second, we can use lidar attenuation to assess changes in cloud optical depth, which is a strong control on cloud albedo (Twomey, 1977). Lidar attenuation is the best available measure of cloud optical depth from CALIPSO. Figure 12c shows no difference in attenuation over open water or over sea ice during summer. While we do not have the actual values for cloud optical depth over open water or over sea ice, observations show no evidence that summer clouds are becoming optically thicker in response to sea ice loss. Because summer clouds are insensitive to changes in sea ice cover, the surface-albedo feedback, one of the dominant feedbacks driving amplified Arctic warming (Pithan & Mauritsen, 2014), is likely unabated.

6. Conclusions

Due largely to recent record-breaking sea ice minima, there has been pronounced variability in Arctic sea ice cover over the last decade. Motivated by this large variability in Arctic sea ice cover, we investigated the influence of sea ice cover on liquid clouds during summer and fall. While this study is not the first to explore cloud-sea ice relationships over the last decade (Barton et al., 2012; Kay et al., 2008; Kay & Gettelman, 2009; Liu et al., 2012; Palm et al., 2010; Sato et al., 2012; Schweiger et al., 2008; Taylor et al., 2015; Wu & Lee, 2012), our results provide new insights into cloud-sea ice relationships that were not available in previous analyses. Specifically, our use of the intermittent mask restricts our analysis to the regions of the Arctic Ocean where sea ice concentration varies, thereby enabling us to isolate the influence of sea ice cover on clouds. Notably, in all 8 years from 2008 to 2015, we find no influence of sea ice cover on summer clouds and a strong influence of sea ice cover on fall clouds. The intermittent mask method also indicates that sea ice cover may also be a strong influence on spring and winter clouds because the air-sea coupling hypothesis supports a cloud response to sea ice loss in all nonsummer seasons. Our results identify the cloud response to sea ice variability and support the local air-sea coupling hypothesis. Summer liquid clouds do not respond to summer sea ice loss. In contrast, liquid clouds do respond to sea ice loss during nonsummer seasons: more liquid clouds form over open water than over sea ice.

Acknowledgments
AcknowledgementsThis work was supported by a NASA grant (12-CCST10-0095 from proposal number NNX14AB35G), the Centre National d'Études Spatiales (CNES), and by the Université Pierre et Marie Curie. A.L.M. was also supported by the Chateaubriand Fellowship of the Office for Science & Technology of the Embassy of France in the United States. The CALIPSO-GOCCP cloud and sea ice data were uploaded from the ClimServ center (http://climserv.ipsl.polytechnique.fr/). The input files and analysis code necessary to produce the results are available at sftp://arielm@cheyenne.ucar.edu upon request. Data requests should be addressed to ariel.morrison@colorado.edu. The authors thank M. Serreze, M. Shupe, W. Abdalati, and P. Taylor for their helpful comments on the manuscript and the statistical tests. We declare no competing financial interests.

References

Abbot, D. S., & Tziperman, E. (2009). Controls on the activation and strength of a high latitude Convective Cloud Feedback. *Journal of the Atmospheric Sciences*, *66*(2), 519–529. https://doi.org/10.1175/2008JAS2840.1

Agnew, T. A., & Howell, S. (2003). The use of operational ice charts for evaluating passive microwave ice concentration data. *Atmosphere-Ocean*, *41*(4), 317–331. https://doi.org/10.3137/ao.410405

Andreas, E. L., Guest, P. S., Persson, P. O. G., Fairall, C. W., Horst, T. W., Moritz, R. E., & Semmer, S. R. (2002). Near-surface water vapor over polar sea ice is always near ice saturation. *Journal of Geophysical Research*, *107*(C10), 8033. https://doi.org/10.1029/2000JC000411

Barton, N. P., Klein, S. A., Boyle, J. S., & Zhang, Y. Y. (2012). Arctic synoptic regimes: Comparing domain-wide Arctic cloud observations with CAM4 and CAM5 during similar dynamics. *Journal of Geophysical Research*, *117*, D15205. https://doi.org/10.1029/2012JD017589

Bindoff, N. L., Stott, P. A., AchutaRao, K. M., Allen, M. R., Gillett, N., Gutzler, D., … Zhang, X. (2013). Detection and attribution of climate change: From global to regional. In T. F. Stocker, et al. (Eds.), *Climate change 2013: The physical science basis. Contribution of Working Group I to the Fifth Assessment Report of the Intergovernmental Panel on Climate Change* (pp. 867–952). Cambridge University Press. https://doi.org/10.1017/CBO9781107415324.022

Bitz, C. M., Holland, M. M., Hunke, E., & Moritz, R. E. (2005). Maintenance of the sea-ice edge. *Journal of Climate*, *18*, 2903–2921.

Boisvert, L. N., & Stroeve, J. C. (2015). The Arctic is becoming warmer and wetter as revealed by the Atmospheric Infrared Sounder. *Geophysical Research Letters*, *42*, 4439–4446. https://doi.org/10.1002/2015GL063775

Boisvert, L. N., Wu, D. L., & Shie, C.-L. (2015). Increasing evaporation amounts seen in the Arctic between 2003 and 2013 from AIRS data. *Journal of Geophysical Research: Atmospheres*, *120*, 6865–6881. https://doi.org/10.1002/2015JD023258

Bony, S., Stevens, B., Frierson, D. M. W., Jakob, C., Kageyama, M., Pincus, R., … Webb, M. J. (2015). Clouds, circulation and climate sensitivity. *Nature Geoscience*, *8*(4), 261–268. https://doi.org/10.1038/ngeo2398

Breivik, L.-A., Eastwood, S., Godøy, Ø., Schyberg, H., Andersen, S., & Tonboe, R. (2001). Sea ice products for EUMETSAT satellite application facility. *Canadian Journal of Remote Sensing*, *27*(5), 403–410. https://doi.org/10.1080/07038992.2001.10854883

Cesana, G., & Chepfer, H. (2013). Evaluation of the cloud thermodynamic phase in a climate model using CALIPSO-GOCCP. *Journal of Geophysical Research: Atmospheres*, *118*, 7922–7937. https://doi.org/10.1002/jgrd.50376

Cesana, G., Chepfer, H., Winker, D., Getzewich, B., Cai, X., Jourdan, O., … Reverdy, M. (2016). Using in situ airborne measurements to evaluate three cloud phase products derived from CALIPSO. *Journal of Geophysical Research: Atmospheres*, *121*(10), 5788–5808. https://doi.org/10.1002/2015JD024334

Cesana, G., Kay, J. E., Chepfer, H., English, J. M., & de Boer, G. (2012). Ubiquitous low-level liquid-containing Arctic clouds: New observations and climate model constraints from CALIPSO-GOCCP. *Geophysical Research Letters*, *39*, L20804. https://doi.org/10.1029/2012GL053385

Chepfer, H., Bony, S., Winker, D., Cesana, G., Dufresne, J. L., Minnis, P., … Zeng, S. (2010). The GCM-oriented CALIPSO cloud product (CALIPSO-GOCCP). *Journal of Geophysical Research*, *115*, D00H16. https://doi.org/10.1029/2009JD012251

Chepfer, H., Cesana, G., Winker, D., Getzewich, B., Vaughan, M., & Liu, Z. (2013). Comparison of two different cloud climatologies derived from CALIOP-attenuated backscattered measurements (level 1): The CALIPSO-ST and the CALIPSO-GOCCP. *Journal of Atmospheric and Oceanic Technology*, *30*, 725–744.

Curry, J. A., Schramm, J. L., & Ebert, E. E. (1993). Impact of clouds on the surface radiation balance of the Arctic Ocean. *Meteorology and Atmospheric Physics*, *51*, 197–217.

de Boer, G., Shupe, M. D., Caldwell, P. M., Bauer, S. E., Persson, O., Boyle, J. S., … Tjernström, M. (2014). Near-surface meteorology during the Arctic Summer Cloud Ocean Study (ASCOS): Evaluation of reanalyses and global climate models. *Atmospheric Chemistry and Physics*, *14*(1), 427–445. https://doi.org/10.5194/acp-14-427-2014

Dee, D. P., Uppala, S. M., Simmons, A. J., Berrisford, P., Poli, P., & Kobayashi, S. (2011). The ERA-Interim reanalysis: Configuration and performance of the data assimilation system. *Quarterly Journal of the Royal Meteorological Society*, *137*, 553–597.

Dufresne, J.-L., & Bony, S. (2008). An assessment of the primary sources of spread of global warming estimates from coupled atmosphere-ocean models. *Journal of Climate*, *21*, 5135–5144.

Fetterer, F., Knowles, K., Meier, W., & Savoie, M. (2002). Sea Ice Index, Boulder, Colorado USA, National Snow and Ice Data Center (updated daily).

Ganeshan, M., & Wu, D. L. (2016). The open-ocean sensible heat flux and its significance for Arctic boundary layer mixing during early fall. *Atmospheric Chemistry and Physics*, *16*, 13,173–13,184. https://doi.org/10.5194/acp-16-13173-2016

Guzman, R., Chepfer, H., Noel, V., Vaillant de Guélis, T., Kay, J. E., Raberanto, P., … Winker, D. M. (2017). Direct atmosphere opacity observations from CALIPSO provide new constraints on cloud-radiation interactions. *Journal of Geophysical Research: Atmospheres*, *122*, 1066–1085. https://doi.org/10.1002/2016JD025946

Intrieri, J. M., Fairall, C. W., Shupe, M. D., Persson, P. O. G., Andreas, E. L., Guest, P. S., & Moritz, R. E. (2002). An annual cycle of Arctic surface cloud forcing at SHEBA. *Journal of Geophysical Research*, *107*(C10), 8039. https://doi.org/10.1029/2000JC000439

Intrieri, J. M., Shupe, M. D., Uttal, T., & McCarty, B. J. (2002). An annual cycle of Arctic cloud characteristics observed by radar and lidar at SHEBA. *Journal of Geophysical Research*, *107*(C10), 8030. https://doi.org/10.1029/2000JC000423

Kay, J. E., & Gettelman, A. (2009). Cloud influence on and response to seasonal Arctic sea ice loss. *Journal of Geophysical Research: Atmospheres*, *114*, D18204. https://doi.org/10.1029/2009JD011773

Kay, J. E., Holland, M. M., & Jahn, A. (2011). Inter-annual to multi-decadal Arctic sea ice extent trends in a warming world. *Geophysical Research Letters*, *38*, L15708. https://doi.org/10.1029/2011GL048008

Kay, J. E., & L'Ecuyer, T. (2013). Observational constraints on Arctic Ocean clouds and radiative fluxes during the early 21st century. *Journal of Geophysical Research: Atmospheres*, *118*, 7219–7236. https://doi.org/10.1002/jgrd.50489

Kay, J. E., L'Ecuyer, T., Chepfer, H., Loeb, N., Morrison, A., & Cesana, G. (2016). Recent advances in Arctic cloud and climate research. *Current Climate Change Reports*, *2*(4), 159–169. https://doi.org/10.1007/s40641-016-0051-9

Kay, J. E., Shupe, M. D., Uttal, T., & McCarty, B. J. (2008). The contribution of cloud and radiation anomalies to the 2007 Arctic sea ice extent minimum. *Geophysical Research Letters*, *35*, L08503. https://doi.org/10.1029/2000JC000423

Kirchmeier-Young, M. C., Zwiers, F. W., & Gillett, N. P. (2017). Attribution of extreme events in Arctic sea ice extent. *Journal of Climate*, *30*, 553–571.

Klein, S. A., & Hartmann, D. L. (1993). The seasonal cycle of low stratiform clouds. *Journal of Climate*, *6*, 1587–1606.

Lacour, A., Chepfer, H., Shupe, M. D., Miller, N. B., Noel, V., Kay, J. E., … Guzman, R. (2017). Greenland clouds observed in CALIPSO-GOCCP: Comparison with ground-based Summit observations. *Journal of Climate*, *30*, 6065–6083. https://doi.org/10.1175/JCLI-D-16-0552.1

Liu, Y., Key, J. R., Liu, Z., Wang, X., & Vavrus, S. J. (2012). A cloudier Arctic expected with diminishing sea ice. *Geophysical Research Letters*, *39*, L05705. https://doi.org/10.1029/2012GL051251

Liu, Z., Marchand, R., & Ackerman, T. (2010). A comparison of observations in the tropical western Pacific from ground-based and satellite millimeter-wavelength cloud radars. *Journal of Geophysical Research*, *115*, D24206. https://doi.org/10.1029/2009JD013575

Marchand, R., Beagley, N., Thompson, S. E., Ackerman, T. P., & Schultz, D. M. (2006). A bootstrap technique for testing the relationship between local-scale radar observations of cloud occurrence and large-scale atmospheric fields. *Journal of the Atmospheric Sciences*, *63*, 2813–2830.

Matus, A. V., & L'Ecuyer, T. (2017). The role of cloud phase in Earth's radiation budget. *Journal of Geophysical Research: Atmospheres*, *122*, 2559–2578. https://doi.org/10.1002/2016JD025951

Min, S.-K., Zhang, X., Zwiers, F. W., & Agnew, T. (2008). Human influence on Arctic sea ice detectable from early 1990s onwards. *Geophysical Research Letters*, *35*, L21701. https://doi.org/10.1029/2008GL035725

Morrison, H., de Boer, G., Feingold, G., Harrington, J., Shupe, M. D., & Sulia, K. (2012). Resilience of persistent Arctic mixed-phase clouds. *Nature Geoscience*, *5*, 11–17.

Nolin, A. W., Armstrong, R., & Maslanik, J. (1998). Near-real-time SSM/I-SSMIS EASE-grid daily global ice concentration and snow extent, Version 4, [06/01/2008–11/30/2015], Boulder, Colorado USA, NASA National Snow and Ice Data Center Distributed Active Archive Center, https://doi.org/10.5067/VF7QO90IHZ99, Accessed. 04/30/2016

Norris, J. R., Allen, R. J., Evan, A. T., Zelinka, M. D., O'Dell, C. W., & Klein, S. A. (2016). Evidence for climate change in the satellite cloud record. *Nature*, *536*, 72–75.

Palm, S. P., Strey, S. T., Spinhirne, J., & Markus, T. (2010). Influence of Arctic sea ice extent on polar cloud fraction and vertical structure and implications for region climate. *Journal of Geophysical Research*, *40*, D21209. https://doi.org/10.1029/2010JD013900

Persson, P. O. G. (2012). Onset and end of the summer melt season over sea ice: Thermal structure and surface energy perspective from SHEBA. *Climate Dynamics*, *39*, 1349–1371. https://doi.org/10.1007/s00382-011-1196-9

Pithan, F., & Mauritsen, T. (2014). Arctic amplification dominated by temperature feedbacks in contemporary climate models. *Nature Geoscience*, *7*, 181–184.

Rayner, N. A., Parker, D. E., Horton, E. B., Folland, C. K., Alexander, L. V., Rowell, D. P., … Kaplan, A. (2003). Global analyses of sea surface temperature, sea ice, and night marine air temperature since the late nineteenth century. *Journal of Geophysical Research*, *108*(D14), 4407. https://doi.org/10.1029/2002JD002670

Sato, K., Inoue, J., Kodama, Y.-M., & Overland, J. E. (2012). Impact of Arctic sea-ice retreat on the recent change in cloud-based height during autumn. *Geophysical Research Letters*, *39*, L10503. https://doi.org/10.1029/2012GL051850

Schafer, M., Bierwirth, E., Ehrlich, A., Jacket, E., Werner, F., & Wendisch, M. (2017). Directional, horizontal inhomogeneities of cloud optical thickness fields retrieved from ground-based and airborne spectral imaging. *Atmospheric Chemistry and Physics*, *17*, 2359–2372.

Schweiger, A. J., Lindsay, R. W., Vavrus, S., & Francis, J. A. (2008). Relationships between Arctic sea ice and clouds during autumn. *Journal of Climate*, *21*, 4799–4810.

Screen, J. A., & Simmonds, I. (2010). The central role of diminishing sea ice in recent Arctic temperature amplification. *Nature*, *464*, 1334–1337.

Sedlar, J., Tjernström, M., Mauritsen, T., Shupe, M. D., Brooks, I. M., Persson, P. O. G., … Nicolaus, M. (2011). A transitioning Arctic surface energy budget: the impacts of solar zenith angle, surface albedo and cloud radiative forcing. *Climate Dynamics*, *37*, 1643–1660.

Serreze, M. C., & Barrett, A. P. (2011). Characteristics of the Beaufort Sea high. *Journal of Climate*, *24*, 159–182.

Serreze, M. C., Barrett, A. P., Stroeve, J. C., Kindig, D. N., & Holland, M. M. (2009). The emergence of surface-based Arctic amplification. *The Cryosphere*, *3*, 11–19.

Serreze, M. C., Carse, F., Barry, R. G., & Rogers, J. C. (1997). Icelandic low cyclone activity: Climatological features, linkages with the NAO, and relationships with recent changes in the Northern Hemisphere circulation. *Journal of Climate*, *10*, 453–464.

Shupe, M. D., & Intrieri, J. M. (2004). Cloud radiative forcing of the Arctic surface: The influence of cloud properties, surface albedo, and solar zenith angle. *Journal of Climate*, *17*, 616–628.

Shupe, M. D., Matrosov, S. Y., & Uttal, T. (2006). Arctic mixed-phase cloud properties derived from surface-based sensors at SHEBA. *Journal of the Atmospheric Sciences*, *63*, 697–711.

Shupe, M. D., Persson, P. O. G., Brooks, I. M., Tjernström, M., Sedlar, J., Mauritsen, T., … Leck, C. (2013). Cloud and boundary layer interactions over the Arctic sea-ice in late summer. *Atmospheric Chemistry and Physics*, *13*, 9379–9400. https://doi.org/10.5194/acp-13-9379-2013

Sotiropoulou, G., Tjernström, M., Sedlar, J., Achtert, P., Brooks, B. J., Brooks, I. M., … Wolfe, D. (2016). Atmospheric conditions during the Arctic clouds in summer experiment (ACSE): Contrasting open water and sea ice surfaces during melt and freeze-up seasons. *Journal of Climate*, *29*, 8721–8744.

Stroeve, J. C., Serreze, M. C., Holland, M., Kay, J. E., Malanik, J., & Barrett, A. P. (2012). The Arctic's rapidly shrinking sea ice extent: A research synthesis. *Climatic Change*, *110*, 1005–1027.

Strong, C., & Rigor, I. G. (2013). Arctic marginal ice zone trending wider in summer and narrower in winter. *Geophysical Research Letters*, *40*, 4864–4868. https://doi.org/10.1002/grl.50928

Stubenrauch, C. J., Rossow, W. B., Kinne, S., Ackerman, S., Cesana, G., Chepfer, H., … Zhao, G. (2013). Assessment of global cloud datasets from satellites: project and database initiated by the GEWEX radiation panel. *Bulletin of the American Meteorological Society*, *94*, 1031–1049.

Taylor, P. C., Kato, S., Xu, K.-M., & Cai, M. (2015). Covariance between Arctic sea ice and clouds within atmospheric state regimes at the satellite footprint level. *Journal of Geophysical Research: Atmospheres*, *120*, 12,656–12,678. https://doi.org/10.1002/2015JD023520

Thorsen, T. J., Fu, Q., & Comstock, J. (2011). Comparison of the CALIPSO satellite and ground-based observations of cirrus clouds at the ARM TWP sites. *Journal of Geophysical Research*, *116*, D21203. https://doi.org/10.1029/2011JD015970

Tjernström, M., Shupe, M. D., Brooks, I. M., Persson, P. O. G., Prytherch, J., Salisbury, D. J., … Wolfe, D. (2015). Warm-air advection, air mass transformation and fog causes rapid ice melt. *Geophysical Research Letters*, *42*, 5594–5602. https://doi.org/10.1002/2015GL064373

Tompkins, A. M., & di Giuseppe, F. (2015). An interpretation of cloud overlap statistics. *Journal of the Atmospheric Sciences*, *72*, 2877–2889.

Twomey, S. (1977). The influence of pollution on the shortwave albedo of clouds. *Journal of the Atmospheric Sciences*, *34*, 1149–1152.

van de Poll, H. M., Grubb, H., & Astin, I. (2006). Sampling uncertainty properties of cloud fraction estimates from random transect observations. *Journal of Geophysical Research*, *11*, L04701. https://doi.org/10.1029/2006

Verlinde, J., Harrington, J. Y., Yannuzzi, V. T., Avramov, A., Greenberg, S., Richardson, S. J., … Schofield, R. (2007). The mixed-phase Arctic cloud experiment. *Bulletin of the American Meteorological Society*, *88*, 205–221.

Webb, M. J., Lambert, F. H., & Gregory, J. M. (2013). Origins of differences in climate sensitivity, forcing and feedback in climate models. *Climate Dynamics*, *40*, 677–707.

Winker, D. M., Pelon, J., Coakley, J. A. Jr., Ackerman, S. A., Charlson, R. J., Colarco, P. R., … Wielicki, B. A. (2010). The CALIPSO missions: A global 3D view of aerosols and clouds. *Bulletin of the American Meteorological Society*, *9*, 1211–1229.

Wong, S., Fetzer, E. J., Schreier, M., Manipon, G., Fishbein, E. F., Kahn, B. H., … Irion, F. W. (2015). Cloud-induced uncertainties in AIRS and ECMWF temperature and specific humidity. *Journal of Geophysical Research: Atmospheres*, *120*, 1880–1901. https://doi.org/10.1002/2014JD022440

Wu, D. L., & Lee, J. N. (2012). Arctic low cloud changes as observed by MISR and CALIOP: Implication for the enhanced autumnal warming and sea ice loss. *Journal of Geophysical Research*, *117*, D07107. https://doi.org/10.1029/2011JD017050